Identification and lattice location of oxygen impurities in α-Si_3N_4

J. C. Idrobo,[1,2,3,a] M. P. Oxley,[1,2] W. Walkosz,[3] R. F. Klie,[3] S. Öğüt,[3] B. Mikijelj,[4] S. J. Pennycook,[1,2] and S. T. Pantelides[1,2]
[1]*Department of Physics and Astronomy, Vanderbilt University, Nashville, Tennessee 37235, USA*
[2]*Materials Science and Technology Division, Oak Ridge National Laboratory, Oak Ridge, Tennessee 37831, USA*
[3]*Department of Physics, University of Illinois at Chicago, Chicago, Illinois 60607, USA*
[4]*Ceradyne Inc. Costa Mesa, California 92626, USA*

(Received 2 September 2009; accepted 20 September 2009; published online 21 October 2009)

For over 40 years impurities have been believed to stabilize the ceramic α-Si_3N_4 but there is no direct evidence for their identity or lattice location. In bulk materials electron microscopy can generally image heavy impurities. Here we report direct imaging of N columns in α-Si_3N_4 that suggests the presence of excess light elements in specific N columns. First-principles calculations rule out Si or N interstitials and suggest O impurities, which are then confirmed by atomically resolved electron-energy-loss spectroscopy. The result provides a possible explanation for the stability of α-Si_3N_4 with implications for the design of next-generation structural ceramics. © *2009 American Institute of Physics*. [doi:10.1063/1.3250922]

α-silicon nitride (α-Si_3N_4) is a promising material for the next generation of structural ceramics because its strength is similar to that of β-Si_3N_4 and its hardness is surpassed only by boron carbide and diamond.[1] However, α-Si_3N_4 tends to transform into β-Si_3N_4 at high temperatures, which limits its potential uses. It has been known for almost 40 years that the presence of different impurities such as iron or oxygen influence the transformation from α-Si_3N_4 to β-Si_3N_4,[2–6] but no direct evidence verifying the presence and location of any impurities has been available. More specifically, there exists evidence that α-Si_3N_4 grains are covered by a thin oxide layer (of composition close to SiO_2), but no direct evidence of oxygen in the bulk material.

(Scanning) transmission electron microscopy (S/TEM) has the spatial resolution to study materials at the atomic level. The observation and quantification of light elements (such as oxygen) has always been a challenge in *Z*-contrast (annular dark field) imaging due their weak interaction with the electron beam. With the addition of aberration-correction optics, it is now possible to image light elements when they are the stoichiometric constituents of a material, e.g., oxygen in oxides.[7] More recently, aberration-correction optics in conventional TEM has also allowed observation of single Ge atoms located in interstitial positions in bulk Ge.[8] But the detection and quantification of light impurities in a matrix formed by light elements has been elusive.

In this letter we report the use of aberration-corrected STEM and image simulations to detect the presence of excess atoms in particular columns that should contain only N in stoichiometric α-Si_3N_4. The excess intensity is slight, suggesting the presence of light elements, possibly N or O. We then used density functional theory (DFT) to rule out N on energetic grounds and accept O as a candidate. Finally, we used atomically resolved electron-energy-loss spectroscopy (EELS) and found a faint oxygen-*K* edge only when the electron beam is focused on those specific columns. Overall, we demonstrate an unusual synergy between *Z*-contrast imaging, EELS, image simulations, and DFT to detect the presence of light *impurities* in a crystal and identify their chemical character.

The silicon nitride sample was consolidated by uniaxial hot pressing of a finely mixed and dispersed 95% α-Si_3N_4 [specific-surface-area (SSA) of 11 m^2/g] powder with pure SiO_2 (SSA 4 m^2/g, 1000 total ppm metal impurities) powder in a 71/29 weight ratio. The consolidated sample had a density of 2.86 g/cm^3 and was substantially pore-free based on polished optical and SEM micrographs. X-ray powder diffraction and a quantitative Rietvald phase analysis on the material indicated the presence of three crystalline phases: α-Si_3N_4, β-Si_3N_4, and Si_2ON_2, with a percentage weight contribution of $60\pm3\%$, $15\pm1\%$, and $26\pm2\%$, respectively.

Z-contrast STEM images were acquired with a FEI Titan S 80–300 operated at 300 kV and equipped with a CEOS aberration corrector, with an electron beam current of ~60 pA, dwell time of 48 μs per pixel, 29.2 mrad convergence semiangle, and 80 mrad annular dark field detector inner semiangle. EELS were acquired from the same sample in a grain with a thickness of 100 nm in a VG Microscopes HB603U operated at 300 kV and equipped with a Nion aberration corrector. The spectra were collected using a 23 mrad convergence semiangle, ~35 mrad collection semiangle, and with an electron beam current of ~50 pA. An acquisition time of 50 s was used for the spectra collected while scanning the electron probe, and the atomically-resolved EEL spectrum is the result of the sum of nine individual spectra with an acquisition time of 1 s.

In the [0001] crystalline orientation, α-Si_3N_4 has three different nitrogen atomic columns (N1, N2, and N3) that are spatially separated in the image plane with distances larger than 70 pm, which means they can be directly resolved by the FEI Titan S 80–300 kV STEM (Ref. 9) as shown in Fig. 1(b). The α-Si_3N_4 grain shown in Fig. 1(b) has a thickness of 78 nm calculated using the absolute log-ratio method.[10] Bloch-wave *Z*-contrast image simulations were carried out with thermal diffuse scattering accounted for using an Einstein model.[11] Debye–Waller factors were taken from the

[a]Author to whom correspondence should be addressed. Electronic mail: juan.idrobo@vanderbilt.edu.

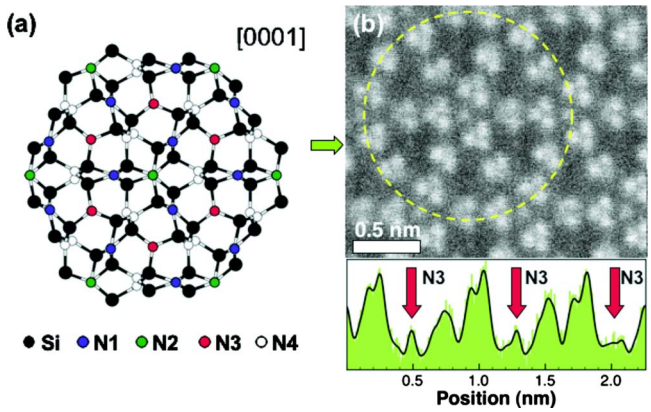

FIG. 1. (Color online) (a) Schematic structure of bulk α-Si_3N_4 in the [0001] crystalline orientation. (b) Annular dark field *Z*-contrast STEM image (raw data) of bulk α-Si_3N_4. Green arrow shows the position in the image where a horizontal intensity line profile was taken (formed by summing over a width of 0.04 nm). Filled (solid line) region in the intensity line profile shows the raw (low-pass filtered) data, respectively. Yellow dashed circumference in (b) highlights the α-Si_3N_4 atomic structure represented in the schematic shown in (a).

literature.[12] The Bloch-wave image simulations [Fig. 2(a)] are in excellent agreement with the measured relative intensities of the N1 and N2 columns. However, the intensity of the N3 column, which has only 50% of the nominal occupancy of N1 and N2 along [0001],[2] is always underestimated by ~25% by the simulations. The discrepancy is present for grains with different thickness. To ensure that the discrepancy between the simulated and measured intensities in the N3 columns is not due to incoherence, we applied various Gaussian and Lorentzian blurs to the images and the intensity ratio between atomic columns changed by less than 2%. Simulations were carried out at various defocus values but the discrepancy remained. We, therefore, conclude that the result is insensitive to the uncertainties in the probe parameters.

We explored the possibility that the extra observed intensity arises from interstitial atoms located along the N3 columns. We performed first-principles calculations based on DFT to obtain the formation energy (FE) of several likely interstitial atoms. We used the projected augmented wave method and a plane-wave basis set implemented in VASP.[13,14] Exchange correlation was included using the generalized gradient-corrected functional given by Perdew.[15] The calculations were performed using a plane-wave energy cutoff of 270 eV and $3\times3\times2$ *k*-points grid. The Si, N, and O interstitial impurities were located between two N atoms along the N3 columns in $1\times1\times2$ and $1\times1\times4$ supercells (containing 57 and 113 atoms, respectively). All the atoms were relaxed until their forces were smaller than 10 meV $Å^{-1}$. The formation energies were calculated using the relation

$$E_{\text{form}} = E_{\text{tot}} - n_j \mu_{\alpha Si_3N_4} - n_i \mu_i,$$

where E_{tot} is the calculated total energy of α-Si_3N_4 with impurities, n_j and n_i are the total number of unit cells of bulk α-Si_3N_4 and number of impurities, respectively.[16] $\mu_{\alpha Si_3N_4}$ and μ_i are the corresponding chemical potentials of bulk α-Si_3N_4 and the impurities, respectively. The chemical potentials for Si, N, and O were defined such that $\mu_{\text{si}}=\mu_{\text{Si-bulk}}$, $\mu_{\text{N}}=\mu_{(1/2)\text{N}}$, and $\mu_{\text{O}}=\mu_{(1/2)\text{O}}$, respectively. These values correspond to the upper limit of the Si, N, and O chemical potentials and therefore the interstitial formation energies are the lowest. We found that interstitial N and Si atoms, one N or Si atom every four N3 atoms (equivalent to a total overall concentration of 1.8%), have a large FE of 5.0 and 6.1 eV, respectively. For the same concentration, interstitial oxygen has a FE of only 1.0 eV. Doubling the oxygen concentration to 3.6% (one O every two N3 atoms) increases the FE to 2.2 eV. The N3 column intensity increases with the oxygen concentration for the simulated images, to the level of reaching a similar overall agreement with experiment obtained for the N1 and N2 columns.

In order to test the hypothesis that O impurities are responsible for the excess intensity, we collected EEL spectra while scanning the electron probe across an area 1×1 nm^2 and did not find any trace of an O signal, indicating that there is no oxide layer covering the surface of the grain [Fig. 2(b), black curve]. But when the electron probe is focused in one of the N3 columns, we detected a trace of the O K edge [Fig. 2(b), red curve].

We note that the oxygen/nitrogen concentration ratio of the N3 columns calculated from the experimental EEL N and O *K*-edge signals of Fig. 2(b) is only about 10%, while the concentration of O/N atoms along the N3 columns used in the DFT calculations and image simulations is 25% (one O for every four N3 atoms) and 50% (one O for every two N3 atoms). To address the apparent discrepancy, we also performed EELS image simulations.[11,17] The images were calculated such that only the inelastic scattering contribution arising from a particular N column (N1, N2, N3, and N4) were taken into account while keeping intact the elastic scattering contribution of all the N and Si atoms. The simulated spectrum images are shown in Fig. 3. It can clearly be observed in Fig. 3 that the N *K*-edge signal coming from N1 and N4 atomic columns is more delocalized with respect to the N2 and N3 atomic columns. This is due to channeling effects arising from the close proximity of the N1 and N4 atomic columns to Si atomic columns. It can also be observed that the N *K*-edge signal coming from the N3 columns is lower when compared with the other N atomic columns. In fact, we find that for bulk α-Si_3N_4, without oxygen impurities, the calculated integrated N *K*-edge signal at the N3 column has only a 27% contribution from the N atoms along the N3 column. The result indicates that the N3 column has a weak electron channeling effect for the incident electrons. When oxygen is incorporated along the N3 with a concentration of 50%, we find that the integrated *K*-edge

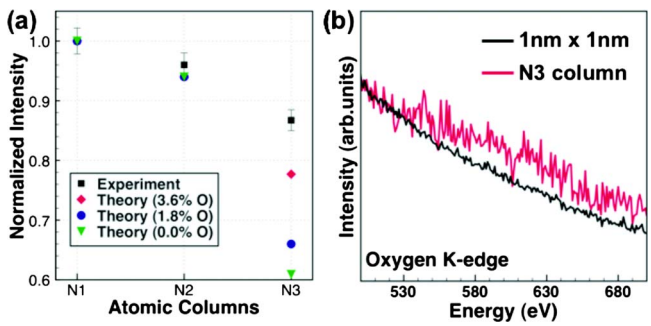

FIG. 2. (Color online) (a) Normalized intensities of the N1, N2, and N3 atomic columns for the experimental and Bloch-wave simulated images. (b) EELS obtained from a 1×1 nm^2 area and a single N3 column showing oxygen present in the N3 column.

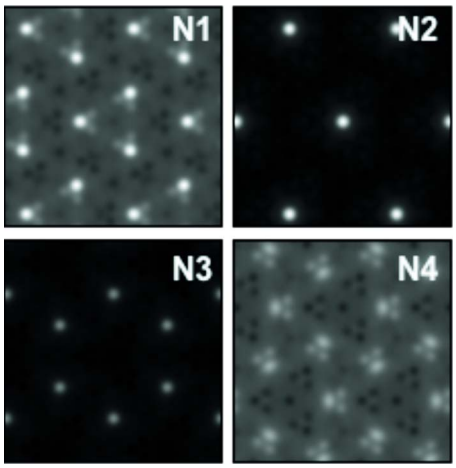

FIG. 3. (Color online) Simulated N *K*-edge spectrum images of bulk α-Si_3N_4. The images were calculated such that only the inelastic scattering contribution arising from a particular N column (N1, N2, N3, and N4) were taken into account while keeping intact the elastic scattering contribution of all the N and Si atoms. The intensity of the spectrum images has been normalized with respect to the minimum and maximum signal coming from the N1 atomic columns.

signal O/N ratio obtained from the EELS image simulations is 16% and therefore in satisfactory agreement with the experimental value.

In summary, we report the use of aberration-corrected STEM and image simulations to detect the presence of excess atoms in particular columns that should contain only N in stoichiometric α-Si_3N_4. The excess intensity is slight, suggesting light elements, possibly N or O. We then used DFT to rule out N on energetic grounds and accept O as a candidate. Finally, we used atomically resolved EELS and found a faint oxygen-*K* edge only when the electron beam is focused on those specific columns. We observed consistently a larger number of α-Si_3N_4 than β-Si_3N_4 grains in the sample studied. Since oxygen is always present in the sintering process and our studies show that oxygen indeed segregates into the bulk of α-Si_3N_4, we infer that oxygen is likely to play a role in the stabilization of α-Si_3N_4.

This research was partially supported by the National Science Foundation under Grant Nos. DMR-0605964 (J.C.I., W.W., and S.O.) and DMR-0513048 (J.C.I.), the Office of Basic Energy Sciences, Division of Materials Sciences and Engineering, U.S. Department of Energy (M.P.O. and S.J.P.), the SHaRE User Facility, which is sponsored by the Division of Scientific User Facilities, Office of Basic Energy Sciences, U.S. Department of Energy, and by the McMinn Endowment (S.T.P.) at Vanderbilt University. Computations were supported by the National Center for Supercomputing Applications.

[1] I.-W. Chen and A. Rosenflanz, Nature (London) **789**, 701 (1997).
[2] S. Wild, P. Grieveson, and K. H. Jack, Spec. Ceram. **5**, 385 (1972).
[3] D. Campos-Loriz and F. L. Riley, J. Mater. Sci. **13**, 1125 (1978).
[4] C.-M. Wang, X. Pan, M. Rühle, F. L. Riley, and M. Mitomo, J. Mater. Sci. **31**, 5281 (1996).
[5] M. Peuckert and P. Greil, J. Mater. Sci. **22**, 3717 (1987).
[6] K. O. Okada, K. Fukuyama, and Y. Kameshima, J. Am. Ceram. Soc. **78**, 2021 (1995).
[7] N. Shibata, M. F. Chisholm, A. Nakamura, S. J. Pennycook, T. Yamamoto, and Y. Ikuhara, Science **316**, 82 (2007).
[8] D. Alloyeau, B. Freitag, S. Dag, L. W. Wang, and C. Kisielowski, Phys. Rev. B **80**, 014114 (2009).
[9] A. Lupini, A. Y. Borisevich, J. C. Idrobo, H. M. Christen, M. Biegalski, and S. J. Pennycook, Microsc. Microanal. **15**, 441 (2009).
[10] R. F. Egerton, *Electron Energy-Loss Spectroscopy in the Electron Microscope*, 2nd ed. (Plenum, New York, 1996).
[11] L. J. Allen, S. D. Findlay, M. P. Oxley, and C. J. Rossouw, Ultramicroscopy **96**, 47 (2003).
[12] H. Toraya, J. Appl. Crystallogr. **33**, 95 (2000).
[13] G. Kresse and J. Furthmüller, Comput. Mater. Sci. **6**, 15 (1996).
[14] P. E. Blöchl, Phys. Rev. B **50**, 17953 (1994).
[15] J. P. Perdew, Phys. Rev. B **33**, 8822 (1986).
[16] C. G. Van de Walle, D. B. Laks, G. F. Neumark, and S. T. Pantelides, Phys. Rev. B **47**, 9425 (1993).
[17] M. P. Oxley and L. J. Allen, Phys. Rev. B **57**, 3273 (1998).